Journal of Theoretical Biology 269 (2011) 138–149

Contents lists available at ScienceDirect

Journal of Theoretical Biology

journal homepage: www.elsevier.com/locate/yjtbi

Cancer stem cell, niche and EGFR decide tumor development and treatment response: A bio-computational simulation study

Xiuwei Zhu [a,b], Xiaobo Zhou [b,*], Michael T. Lewis [c], Ling Xia [a], Stephen Wong [b]

[a] Key Laboratory of Biomedical Engineering of Ministry of Education, Department of Biomedical Engineering, Zhejiang University, Hangzhou 310027, China
[b] Center for Bioengineering and Informatics, The Methodist Hospital Research Institute & Cornell University, Houston, TX 77030, USA
[c] Baylor College of Medicine Breast Center and the Department of Molecular and Cellular Biology, Houston, TX 77030, USA

ARTICLE INFO

Article history:
Received 30 November 2009
Received in revised form
11 October 2010
Accepted 11 October 2010
Available online 20 October 2010

Keywords:
Mathematical model
Compartment method
Signaling pathway
Breast cancer
Tyrosine kinase inhibitors

ABSTRACT

Recent research in cancer biology has suggested the hypothesis that tumors are initiated and driven by a small group of cancer stem cells (CSCs). Furthermore, cancer stem cell niches have been found to be essential in determining fates of CSCs, and several signaling pathways have been proven to play a crucial role in cellular behavior, which could be two important factors in cancer development. To better understand the progression, heterogeneity and treatment response of breast cancer, especially in the context of CSCs, we propose a mathematical model based on the cell compartment method. In this model, three compartments of cellular subpopulations are constructed: CSCs, progenitor cells (PCs), and terminal differentiated cells (TCs). Moreover, (1) the cancer stem cell niche is, considered by modeling its effect on division patterns (symmetric or asymmetric) of CSCs, and (2) the EGFR signaling pathway is integrated by modeling its role in cell proliferation, apoptosis. Our simulation results indicate that (1) a higher probability for symmetric division of CSC may result in a faster expansion of tumor population, and for a larger number of niches, the tumor grows at a slower rate, but the final tumor volume is larger; (2) higher EGFR expression correlates to tumors with larger volumes while a saturation function is observed, and (3) treatments that inhibit tyrosine kinase activity of EGFR may not only repress the tumor volume, but also decrease the CSCs percentages by shifting CSCs from symmetric divisions to asymmetric divisions. These findings suggest that therapies should be designed to effectively control or eliminate the symmetric division of CSCs and to reduce or destroy the CSC niches.

1. Introduction

There is an increasing evidence that a variety of cancers, including those of breast, may be driven by a component of tumor-initiating cells (TIC, also known as cancer stem cells, CSC) that retain stem cell-like properties (Clarke et al., 2006; Reya et al., 2001; Visvader and Lindeman, 2008). These properties include self-renewal, which drives tumor initiation and growth, as well as differentiation, which contributes to cellular heterogeneity of tumors. CSCs are also thought to be able to divide either symmetrically into two identical daughter CSCs or asymmetrically into one daughter CSC and one more differentiated cell (Al-Hajj and Clarke, 2004; Shipitsin et al., 2007). Although the amount of CSCs in a tumor population is relatively small, and maybe comprises 1–5% of primary tumors (Kopper and Hajdu, 2004; Korkaya et al., 2008), CSCs are suggested to account for the therapeutic refractoriness and subsequently the recurrence of cancer, due to their increased detoxification, repair pathways and mutations that lead to failure of apoptosis (Gordan et al., 2007; Gustafsson et al., 2005; Hu et al., 2003; Woodward et al., 2007). Indeed, the CSC hypothesis provides an explanation for the failure of conventional treatments, which are currently designed to kill the rapidly proliferating cells that make up the bulk of tumor cells (Baumann et al., 2008; Boman et al., 2007).

Currently, it is widely accepted that the stem cell's fate is at least partially dependent on the stem cell niche, which is a particular growth environment, consisting of different cell types and extracellular matrix components (Adams and Scadden, 2006; Scadden, 2006; Walker et al., 2009). Besides the maintenance of stem cells (Visnjic et al., 2004; Xie and Spradling, 2000; Zhang et al., 2003), the niche has also been suggested to play an important role in the determination of stem cell's fate (Bjerknes and Cheng, 1999; Lechler and Fuchs, 2005; Li and Neaves, 2006; Potten et al., 1997). The nutrient and molecules in the niche do not only physically determine the size of stem cell population, but also affect the rate at which the stem cells proliferate (Narbonne and Roy, 2006). The deregulation of the niche leading to an unbalance of proliferation and differentiation may result in both tumorigenesis (Li and Neaves, 2006) and the progression of the cancer. Indeed, it has been suggested that targeting the niche could result in a

* Corresponding author.
E-mail address: xzhou@tmhs.org (X. Zhou).

0022-5193/$ - see front matter © 2010 Elsevier Ltd. All rights reserved.
doi:10.1016/j.jtbi.2010.10.016

reduction of the tumor burden (Anderson, 2007; Calabrese et al., 2007; Joyce, 2005). Feedbacks from both stem cell itself and the environment surrounding the cells have been usually considered in modeling cell population dynamics. For example, Paulus et al. (1992) developed a mathematical model that assumed the self-maintenance and cell cycle activity of the stem cells are controlled by the number of these cells in an autoregulatory fashion, Johnston et al. (2007) discussed two feedback models that could regulate the growth of cell numbers and maintain the equilibrium that is normally observed in the crypt.

Furthermore, enormous experimental evidence indicates that the cellular properties, such as proliferation and death, are closely related to many signaling pathways. For example, many studies suggest a significant correlation between the EGFR signaling pathway and cellular proliferation and survival (Athale and Deisboeck, 2006; Birtwistle et al., 2007; Eladdadi and Isaacson, 2008; Timms et al., 2002). Also, HER2 over-expression drives mammary carcinogenesis, tumor growth and invasion through its effects on normal and malignant mammary stem cells (Korkaya et al., 2008). The activities of some drugs are even directly proportional to the level of HER2 present on tumor cell membrane (Vogel et al., 2002).

Many mathematical models have been proposed to study one or more phases of cancer progression (Anderson and Chaplain, 1998; Araujo and McElwain, 2004; Byrne and Chaplain, 1995; Chaplain et al., 2006; Cristini et al., 2003, 2005; El-Kareh and Secomb, 2003; Frieboes et al., 2009; Holz and Fahr, 2001; Ribba et al., 2006; Sinek et al., 2009; Zheng et al., 2005), including tumor growth, angiogenesis, and drug treatment, with the purpose of better understanding the pathophysiology of cancer, its progression, mechanisms of drug resistance, and the optimization of treatment strategies. Recently, there have been a number of models addressing the control and progression of cancer stem cells (Boman et al., 2007; Ganguly and Puri, 2006; Michor et al., 2005). Indeed, early in 1995, Tomlinson and Bodmer (1995) had published a mathematical model of the relationship between stem cells, semi-differentiated cells and fully differentiated cells in intestinal crypt. Based on this model, d'Onofrio and Tomlinson (2007) developed the first nonlinear model of stem cell-progenitor-differentiated cells by incorporating plausible fluctuation in model parameters and assuming that the parameters depend on the numbers of cells in each state of differentiation.

In order to better understand the progression, heterogeneity and treatment response of breast cancer, specifically in the context of CSCs, we describe a mathematical model by employing a simple compartment method. We also integrated two factors in cancer development, i.e., (1) cancer stem cell niche is considered in this work by modeling its effect on division patterns of CSCs, and (2) the EGFR signaling pathway is involved by modeling its role in cell proliferation, apoptosis and drug response. Then, we performed theoretical treatments targeting these two factors to give some potential strategies for cancer therapy. The following section describes the details of the proposed mathematical model.

2. Material and methods

2.1. Basic model of breast cancer

In this work, we investigated breast cancer by using the compartment method. Recent experimental and clinical data suggests that breast cancer can approximately be separated into three cellular subpopulations, which are corresponding to three main compartments constructed in our basic model: cancer stem cells (CSCs), progenitor cells (PCs), and terminal differentiated cells (TCs). It is possible that each of the three compartments can be further divided into several sub-compartments. In this work, however, we only subdivide the compartment of progenitor cells. The dynamics of these cell populations are simply described by mechanisms shown in Fig. 1. CSCs divide either symmetrically to produce two CSCs or asymmetrically to generate one CSC and one PC. The early PCs divide symmetrically to later PCs whose differentiation capacities are decreased. After several times of division (k in Fig. 1, we use $k=7$ in this work), the latest PCs will lose their differentiation capacity and add to TCs compartment in a rate of D_i. For the TCs, they do not divide, but can be lost from the system through many processes, e.g., apoptosis. Also, we assume that CSCs and PCs will also die at a certain rate. The death rates for CSCs, PCs and TCs are denoted by d_1, d_2 and d_3 as shown in Fig. 1. Note that we take the same death rate and division rate for all the sub-compartments in PC compartments, and they do not self-renew but divide and differentiate.

Taken these together, the dynamics of these types of cell populations can be described by using an ordinary differential equations (ODE) system as follows:

$$\frac{dN_{CSC}}{dt} = P_{sy}\omega_{CSC}N_{CSC} - d_1 N_{CSC} \tag{1}$$

$$\frac{dN_{PC_1}}{dt} = P_{asy}\omega_{CSC}N_{CSC} - \omega_{PC}N_{PC_1} - d_2 N_{PC_1} \tag{2a}$$

$$\frac{dN_{PC_i}}{dt} = 2\omega_{PC}N_{PC_{i-1}} - \omega_{PC}N_{PC_i} - d_2 N_{PC_i} \quad (i = 2\ldots k) \tag{2b}$$

$$\frac{dN_{TC}}{dt} = D_i N_{PC_k} - d_3 N_{TC} \tag{3}$$

where N_{CSC} and N_{TC} are the cell numbers of cancer stem cells and tumor cells, N_{PC_i} is the cell number of the ith sub-compartment of PC population. P_{sy} and P_{asy} are the probabilities for symmetric and asymmetric divisions of CSCs. As we assume that CSCs can only divide in these two ways, we have $P_{sy}+P_{asy}=1$. ω_{CSC} and ω_{PC} denote the division rates for CSC and PC. D_i is the differentiation rate from latest PC to TC. d_1, d_2 and d_3 are death rates of CSCs, PCs and TCs, respectively. The parameter k is the number of sub-compartments.

2.2. Integration of stem cell niche

As described above, more and more attention is being attracted to the study of cancer stem cells, and a specific structure, named niche, has been found to support and control the cancer stem cells. To incorporate the niche into our mathematical model, we summarized the relationship between the CSCs and their niche as follows:

(1) The niche is a specific anatomic structure for a stem cell, that is, one niche serves one cancer stem cell. CSCs can only reside in their niches where they obtain necessary nutrients and molecules to survive and maintain their stemness (Ho, 2005).

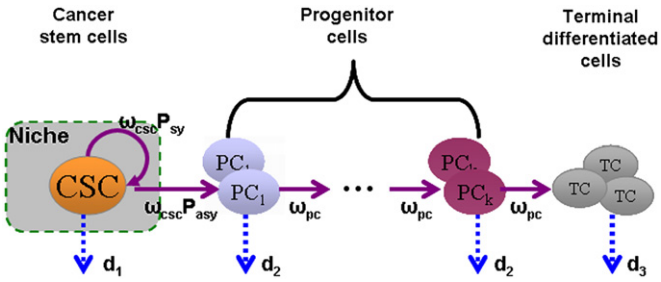

Fig. 1. Schematic representation for the composition in a tumor, including the niche (the gray region in the dashed rectangle) for cancer stem cells. See the text for detailed description.

Once leaving the niche, CSCs will differentiate into PCs and subsequently into TCs. The process of differentiation may be reversible, but we did not consider this case in this work.

(2) Evidence suggests that the number of niches is finite, which could be one reason why there are only a limited number of cancer stem cells in a tumor. While increasing the number of stem cell niches will expand the stem cell population, decreasing the niches will diminish the stem cells, which is supported by recent studies on both normal and abnormal niches (Adams et al., 2007; Li and Neaves, 2006).

(3) Stem cells change from primarily symmetric divisions during early embryonic development to primarily asymmetric divisions in the mid- and late gestation (Morrison and Kimble, 2006). Therefore, the probability of the division pattern (i.e., symmetric or asymmetric) may be dependent on the number of cancer stem cells and the number of niches. As the niches are occupied by more and more cancer stem cells, it is prone to generating differentiated cells, asymmetric division is therefore more likely to undergo.

Based on these points, we integrated the effect of the niche into the system by describing the probability of symmetric division as the function of CSCs and the niche. We modeled the relationship between P_{sy} and N_{CSC} by a simple Boltzmann function:

$$P_{sy}(N_{CSC}) = f(N_{CSC}) = f(N_{niche}) - \frac{f(N_{niche}) - f(0)}{1 + \exp\left(10 \times \frac{N_{CSC}}{N_{niche}} - 5\right)} \quad (4)$$

where N_{niche} is the maximal number of CSCs niches, $f(0)$ is the probability of symmetric division when there is no cancer stem cells, and $f(N_{niche})$ is the probability when all the niches are occupied by cancer stem cells. With these intuitive parameters, we can easily change the relationship between P_{sy} and N_{CSC} by using different values for N_{niche}, $f(0)$ and $f(N_{niche})$. A typical graphical representation and applied parameter values are given in Fig. 2.

2.3. Receptor–ligand interactions

In this section, we discuss the effect of signaling pathways on tumor growth. Eladdadi et al. (2008) proposed a mathematical model that described the relation between cellular proliferation and the numbers of EGRF and HER2 receptors, and the growth factor EGF as well. Their assumption was that the proliferation rate is a function of all the cell surface receptors, which is in turn proportional to the cell density. In a similar way, we incorporated the EGFR pathway into the model (1)–(3) by modeling the effect of receptor–ligand complex on cellular proliferation rates and apoptosis rates. Furthermore, different treatments targeting specific cellular activities were considered as well (Fig. 3).

The biological mechanism of EGFR pathway is indeed complicated. The epidermal growth factor receptor family is composed of four types: EGFR (also called HER1/ErbB-1), HER2 (also known as ErbB-2/neu), HER3 (known as ErbB-3), and HER4 (known as ErbB-4). All these four receptors share an extracellular ligand-binding domain, a single membrane-spanning region, and a cytoplasmic protein tyrosine kinase domain (Eladdadi and Isaacson, 2008). In this work, we used EGFR to represent the whole family for simplification.

Normally, binding of EGF to the extracellular domain of EGFR causes the activation of the receptors and leads to a serial of interactions between activated receptors, recruited proteins, and plasma membrane molecules, finally activating the multiple downstream effectors, which are implicated in the control of proliferation and survival (Birtwistle et al., 2007). However, in the presence of tyrosine kinase inhibitors (TKIs), such as lapatinib, gefitinib, erlotinib, which combine with the intracellular domain of tyrosine kinase activity, the autophosphorylation of receptors will be inhibited and consequently the downstream pathways that are responsible for proliferation and apoptosis remain inactivated (Costa et al., 2007; Gan et al., 2007; Kong et al., 2008). In this case, no matter whether the EGFR is bound by EGF or not, the cascade of the EGFR pathways cannot be stimulated, since the

Parameter	Values
N_{niche}	1000*
$f(0)$	1.0*
$f(N_{niche})$	0.01*
N_{niche}	1500
$f(0)$	0.75
$f(N_{niche})$	0.25

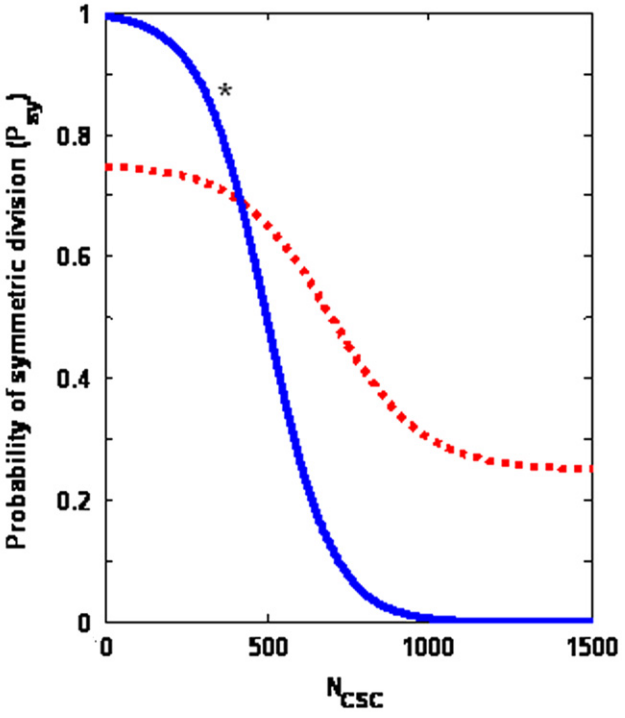

Fig. 2. The relationship between P_{sy} and N_{CSC}. Parameters in Eq. (4) are shown in the table, while the reversed sigmoid curves in the figure give the dependence of P_{sy} on the number of cancer stem cells. Note that the values marked with stars are used for the simulation in this work, while the others are used for illustrating the curve dependence on these parameters.

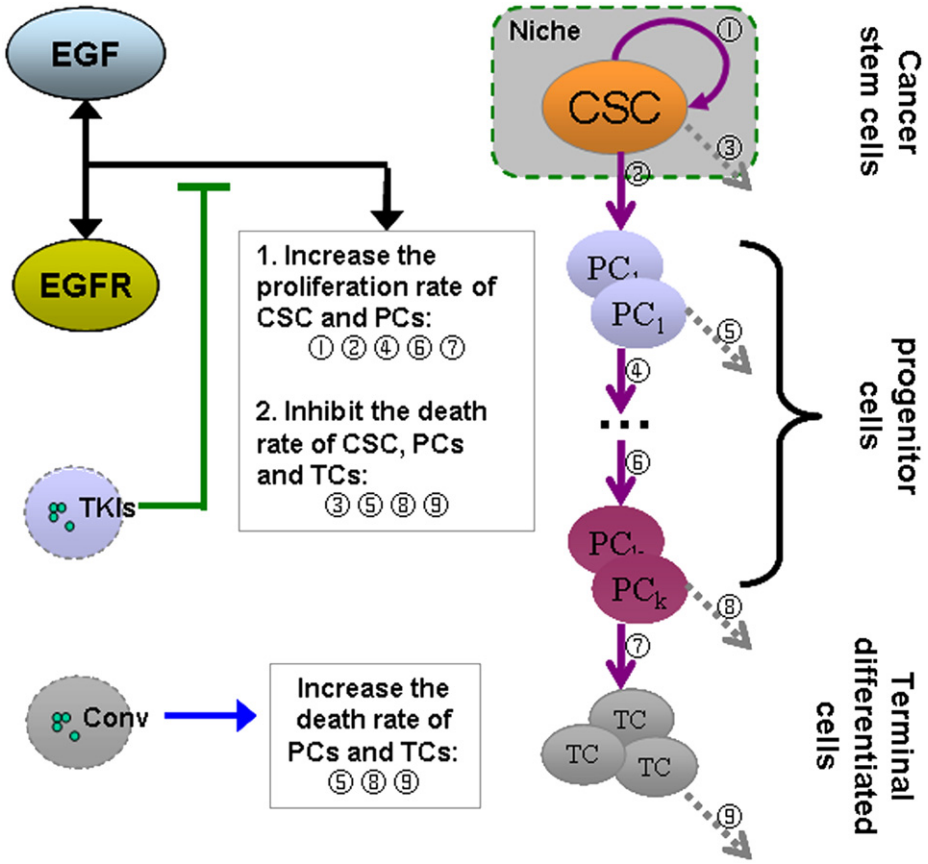

Fig. 3. Schematic representation of the effect of conventional treatment (Conv) and novel treatment (TKIs) on tumor behavior through the EGF–EGFR pathway. While the conventional treatment can only increase the death rate of PCs and TCs, TKIs can both decrease the proliferation rate of CSCs and PCs and increase the death rate of CSCs, PCs and TCs.

signal is blocked due to the failure in activating the intracellular domain of EGFR.

Indeed, there are four states of EGFR, namely: free EGFR, complex EGF–EGFR, EGFR–TKI and EGF–EGFR–TKI. Since only the EGF–EGFR complex is responsible for activation of the EGFR pathway, we just consider the reactions that are related to EGF–EGFR. They can be represented by the following chemical reactions:

$$EGF + EGFR \underset{k_r}{\overset{k_f}{\rightleftharpoons}} EGF:EGFR \tag{5a}$$

$$EGF:EGFR + TKI \underset{k_u}{\overset{k_b}{\rightleftharpoons}} EGF:EFGR:TKI \tag{5b}$$

where Eq. (5a) describes the formation of EGF–EGFR with forward and reverse rate constants k_f and k_r, respectively; Eq. (5b) shows the binding and unbinding processes of TKI to EGF–EGFR with rate constants k_b and k_u, respectively. We consider that these cells are distributed throughout a medium that contains a large amount of EGF ligands. Since the chemical reaction rate is much faster than cellular behavior such as cell proliferation, we use the steady state of Eq. (5) to obtain the concentration of EGF–EGFR. Using the law of Michaelis–Menten kinetics, we derive the quasi-steady-state of EGF–EGFR in Eq. (5a) as

$$[EGF:EGFR] = \frac{[EGFR]_0[EGF]}{K_{m1} + [EGF]} \tag{6}$$

where K_{m1} is a Michaelis constant equal to the substrate concentration, at which the reaction rate is equal to the half of maximum, additionally it can also be defined by $K_{m1} \approx k_r/k_f$. $[EGFR]_0$ is the initial concentration (or the total concentration) of EGFR. Although the receptor numbers may vary due to different gene expression, we assume that in our model, the total number of receptor for the same type of cells is identical.

Since the binding of EGF to the extracellular domain of EGFR and the binding of TKI to the intracellular domain are independent so that they may occur simultaneously without interfering each other. Therefore, for Eq. (5b), the quasi-steady-state of EGF–EGFR–TKI can similarly be calculated as

$$[EGF:EGFR:TKI] = \frac{[EGF:EGFR]_0[TKI]}{K_{m2} + [TKI]} \tag{7}$$

where K_{m2} is the Michaelis constant and $K_{m2} \approx k_b/k_u[EGF{:}EGFR]_0$ is the initial concentration of the complex of EGF and EGFR. In this way, we can derive the effective amount of EGF–EGFR for the activation of downstream factors as follows:

$$[EGF:EGFR]_{eff} = [EGF:EGFR]_0 - [EGF:EGFR:TKI] \tag{8}$$

After obtaining the effective EGF–EGFR, let us now consider how to link it to the cell proliferation rate and apoptosis. It is obvious that a complicated cascade should be activated before the cellular properties are modulated. However, as Monod (1949) and Eladdadi et al. (2008) did, we simply use the Michaelis–Menten kinetics to model the saturated effects of the cell proliferation rate with respect to the EGF–EGFR concentration:

$$\omega_i' = \omega_{max,i}\pi_{act,i}^{EE_{eff}} = \omega_{max,i}\frac{[EGF:EGFR]_{eff}}{\mu_{half} + [EGF:EGFR]_{eff}} \quad (i = CSC,\ PC) \tag{9}$$

where $\omega_{max,i}$ is the maximum cell proliferation rate, μ_{half} is the number of occupied receptors required to generate a half-maximal response. The cell death rates can be modeled by multiplying a

repression function caused by effective EGF:EGFR:

$$d_i' = d_{max,i}\pi_{rep,i}^{EE_{eff}} = d_{max,i}\frac{1}{1+[EGF:EGFR]_{eff}/k_d} \quad (i=1,2,3) \tag{10}$$

where $d_{max,i}$ is the maximum death rate and k_d is a constant for the repression threshold.

Substituting Eqs. (4), (9) and (10) into Eqs. (1)–(3), we can obtain a new ODE system that incorporates the effects of ligand–receptor reactions and stem cell niche into the cellular dynamics of a tumor:

$$\frac{dN_{CSC}}{dt} = P_{sy}(N_{CSC})\omega_{CSC}'N_{CSC} - d_1'N_{CSC} \tag{11}$$

$$\frac{dN_{PC_1}}{dt} = P_{asy}\omega_{CSC}'N_{CSC} - \omega_{PC}'N_{PC_1} - d_2'N_{PC_1} \tag{12a}$$

$$\frac{dN_{PC_i}}{dt} = 2\omega_{PC}'N_{PC_{i-1}} - \omega_{PC}'N_{PC_i} - d_2'N_{PC_i} \quad (i=2\ldots k) \tag{12b}$$

$$\frac{dN_{TC}}{dt} = D_i'N_{PC} - d_3'N_{TC} \tag{13}$$

3. Model analysis

3.1. Parameter settings

The parameters used in this model are listed in Table 1, most of which are based on recent experimental data or scientific literature. The maximal death rates for these three populations were derived from Michor et al.'s work (2005). The maximal division rate for PC cells was estimated using the doubling time of HB4a cell lines $t_{1/2}=48$ h: $\omega_{max,2}=\ln(2)/t_{1/2}=0.0143\ h^{-1}$; no data was available for estimation of $\omega_{max,1}$, we therefore assumed that $\omega_{max,1}=0.5\omega_{max,2}$ based on the findings that CSC divides slower than PC cells. No experimental data was available specifically for the differentiation rate from latest PC to TC (D_i), we therefore used the same value of division rate of PC. The number of receptor complexes required to generate a half-maximal response (μ_{half}) was adopted from Eladdadi et al.'s work. $K_{m1}\approx k_r/k_f$ was calculated using the data from Hendriks et al. (2003). Due to the lack of data available for dynamics of EGFR and TKI interactions, we assumed K_{m2} has the same value for K_{m1}. The initial concentration of the EGF ligand was obtained from Hendriks et al. (2003) and the TKI concentration was set initially with 1.0×10^{-9} M. The total number of receptors per cell was simply the summation of EGFR and HER2 from experimental studies, which varies from 210,000 (normal) to 800,000 (high HER2 expression level) (Eladdadi and Isaacson, 2008). Though the total receptors numbers are assumed to be identical in the same type of cells, experimental data shows that these receptors are found much more in CSCs than in PCs and TCs (Magnifico et al., 2009). Since the cancer stem cell hypothesis states that the tumors are initiated by a small number of CSCs, we selected an initial normalized condition $N_{CSC}=1.0$, with the other two cell populations set to zero. We used the curve shown in Fig. 2 to describe the probability of symmetric division P_{sy} as the function of N_{CSC} and the number of niches.

3.2. Sensitivity analysis

To understand which components of the model contribute most significantly to determining the final tumor volume, here we performed a sensitivity analysis. We took final tumor volume for studying the effects of small variable changes. In each simulation, we recorded the total tumor cells (SCs+PCs+TCs) after the model reached a stable state. Perturbing each parameter from its initial value by 1%, the corresponding percent change in final tumor volume was calculated.

The results of this parameter sensitivity analysis for the proposed model are shown in Fig. 4. From the figure we can see that the system is found to be most sensitive to proliferation rate of CSC ($\omega_{max,1}$) and death rate of PCs ($d_{max,2}$). This suggests that, even very small changes in both the inflow rate of the PC compartment, as represented by growth variable $\omega_{max,1}$, and the outflow rate of the PC compartment, as represented by $d_{max,2}$ here, can affect

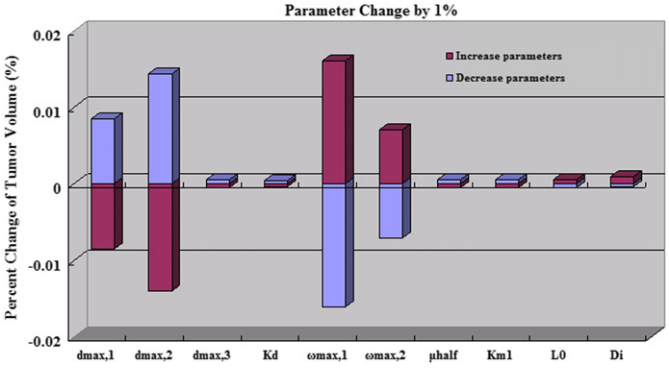

Fig. 4. Sensitivity analysis of the proposed model. This figure shows that the final tumor volume is most sensitive to the proliferation rate of CSC $\omega_{max,1}$, as well as to the death rate of PCs $d_{max,2}$.

Table 1
Parameters for the mathematical model.

Symbols	Values	Physical meaning	Derivation
$d_{max,1}$	0.003/h	Maximal death rate of CSC	MH2005
$d_{max,2}$	0.008/h	Maximal death rate of PC	MH2005
$d_{max,3}$	0.05/h	Maximal death rate of TC	MH2005
k_d	10^7	Constant for repression function	Estimated
$\omega_{max,1}$	0.0072/h	Maximal division rate of CSC	Estimated
$\omega_{max,2}$	0.0143/h	Differentiation rate within PC compartment	EI2008
D_i	0.0143/h	Differentiation rate from latest PC to TC	Estimated
μ_{half}	1300–4800	Number of receptor complexes required to generate a half-maximal response	EI2008
K_{m1}	2.5×10^{-9} M	Michaelis constant for EGF–EGFR steady state	HO2003
K_{m2}	2.5×10^{-9} M	Michaelis constant for EGF–EGFR–TKI steady state	Estimated
L_0	1.6×10^{-9} M	Initial EGF ligand concentration	HO2003
TKI	1.0×10^{-9} M	Initial TKI concentration	Estimated
EGFR	210,000–800,000	Total receptor numbers per cell	EI2008
k	7	Division number of PC	Estimated
P_{sy}	(0, 1)	Probability of symmetric division of CSCs	Estimated

MH2005 represents the paper of Michor et al. (2005); EI2008 represents the paper of Eladdadi and Isaacson (2008); HO2003 represents the paper of Hendriks et al. (2003).

simulation results. The perturbation of D_i shows no significant effect on the system. This would indicate that the whole tumor is largely consisted in PC compartment. Indeed, clinical investigations show that most of the cells in primary tumors are PCs, while CSC comprises only 1–5% (Kopper and Hajdu, 2004; Korkaya et al., 2008). Note that, the percent changes of tumor volume in all cases are less than 0.02%, which shows that the proposed model is very stable.

3.3. Stability analysis

The basic model (1)–(3) describes the development of breast cancer, with the purpose of incorporating the most important concepts while keeping the model as simple as possible. The dynamics of the basic model are very simple, since there is no feedback in this case. In this section, we explored the steady state when there are no treatments. The steady state is reached when the following relationships are satisfied:

$$d_1 = P_{sy}\omega_{CSC} \tag{A1}$$

$$\begin{cases} d_2 = \dfrac{P_{asy}\omega_{CSC}N_{CSC}}{N_{PC_1}} - \omega_{PC} \\ d_2 = \dfrac{2\omega_{PC}N_{PC_{i-1}}}{N_{PC_i}} - \omega_{PC} \end{cases} \Rightarrow \begin{cases} P_{asy} = 2\dfrac{\omega_{PC}}{\omega_{CSC}}\dfrac{N_{PC_1}^2}{N_{CSC}N_{PC_2}} \\ N_{PC_1} = \dfrac{P_{asy}\omega_{CSC}N_{CSC}}{\omega_{PC}+d_2} \\ N_{PC_i} = \left(\dfrac{2\omega_{PC}}{\omega_{PC}+d_2}\right)^{i-1} N_{PC_1} \quad (i=2,\ldots k) \end{cases} \tag{A2}$$

$$d_3 = \frac{\omega_{PC}N_{PC_k}}{N_{TC}} \tag{A3}$$

These equations decide the selection of parameter values. As shown in Table 1, most of the values are derived from other published paper, where there is no source cited, parameters were selected to observe steady-state values. The probability of symmetric division of CSC (P_{sy}) was previously introduced by Paguirigan et al. (2007) and F. Michor' group (Dingli et al., 2007; Michor et al., 2005). However, the precise range of the probability is unclear, we therefore simulated our model by using the value of P_{sy} within the range of (0, 1). When $P_{sy} < d_1/\omega_{CSC}$, the system is unstable until cell population decreases to zero. On the contrary, while $P_{sy} > d_1/\omega_{CSC}$, the system is also unstable, and the output shows an exponential increase in CSC, PCs and TCs. Only on the condition that Eq. (A1) is satisfied, the cell populations can reach a steady state, i.e., the number of cells produced is balanced by the number lost. Here, in the basic model (i.e., when P_{sy} is independent of the number of stem cells N_{CSC}), we can solve the solution easily, i.e., the cell numbers of

$$\begin{aligned} &[CSC, PC_1, \ldots, PC_i, \ldots, PC_{k-1}, PC_k, TC] \\ &= N_{CSC}\left[1, \frac{P_{asy}\omega_{CSC}}{\omega_{PC}+d_2}, \frac{2\omega_{PC}}{\omega_{PC}+d_2}\frac{P_{asy}\omega_{CSC}}{\omega_{PC}+d_2}, \ldots,\right. \\ &\quad \times\left(\frac{2\omega_{PC}}{\omega_{PC}+d_2}\right)^{i-1}\frac{P_{asy}\omega_{CSC}}{\omega_{PC}+d_2}, \ldots, \quad \left(\frac{2\omega_{PC}}{\omega_{PC}+d_2}\right)^{k-2}\frac{P_{asy}\omega_{CSC}}{\omega_{PC}+d_2}, \\ &\quad \times\frac{2\omega_{PC}}{D_i+d_2}\left(\frac{2\omega_{PC}}{\omega_{PC}+d_2}\right)^{k-2}\frac{P_{asy}\omega_{CSC}}{\omega_{PC}+d_2}, \\ &\quad \left.\times\frac{D_i}{d_3}\frac{2\omega_{PC}}{D_i+d_2}\left(\frac{2\omega_{PC}}{\omega_{PC}+d_2}\right)^{k-2}\frac{P_{asy}\omega_{CSC}}{\omega_{PC}+d_2}\right] \end{aligned}$$

Since all the parameters are known, the steady state of all types of cells is only dependent of N_{CSC}. In the advanced model, i.e., when P_{sy} is dependent with the number of stem cells, we can solve the eigenvalues of the system (Eqs. (11)–(13)) as $[P_{sy}\omega_{CSC}-d_1, -\omega_{PC}-d_2(\text{repeated } k \text{ times}), -d_3]$. Therefore, all of the eigenvalues are negative if $P_{sy}\omega_{CSC}-d_1<0$ is satisfied. In this case, the steady state of the system is stable. Since P_{sy} changes with the number of stem cells (N_{CSC}) in the range of (0, 1), we can obviously find a point where $P_{sy}\omega_{CSC}-d_1=0$. At this point, since the form of $P_{sy}(N_{CSC})$ is known (in Eq. (4)), we can solve the cell number of cancer stem cells, i.e.,

$$N_{CSC}^* = \frac{N_{niche}}{10}\ln(-f_0+d_1/\omega_1/f_N-d_1/\omega_1)$$

Then, the other types of cells can also be calculated in the same way as in the basic model. Furthermore, for any $N_{CSC} \subset (0, N_{CSC}^*)$, Eq. (11) >0, then the stem cell number increases to N_{CSC}^*, while for any $N_{CSC} \subset (N_{CSC}^*, \infty)$, the value of Eq. (11) is always negative, which results in a decrease of stem cell number down to N_{CSC}^*. Therefore, the equilibrium of this system is global attractive.

In the following section, we will discuss some results that are simulated with the model described in the previous section. Firstly, we studied the tumor growth where the symmetric division probability is independent of the niches. Then, we considered the effect of the niche on the symmetric division. Next, we simulated and compared the tumor responses to various drug treatments, in order to show the effect of the niches. Also, we compared the simulation results with clinical data obtained from two kinds of drug treatments. Note that for the purpose of convenience, in the following figures we plot the curve for PCs as a summation of all sub-compartments of PCs.

4. Results

4.1. CSC division pattern decides the tumor growth

To study the effect of division patterns of CSCs on tumor growth, we varied the value of P_{sy} from 0 to 1 with a step of 0.05 for the simulation. Note that we assumed the probabilities for symmetric and asymmetric division are constants through the whole simulation in this case. Our simulations showed that at an intermediate value of $P_{sy}(=0.3$ in this case), the tumor volume reached a steady state, while the higher value of the $P_{sy}(>0.3)$ caused the expansion of tumor volume and the lower value of $P_{sy}(<0.3)$ made the tumor diminished (Fig. 5). Since the other parameters were the same as that in Table 1, the simulation variation was caused by P_{sy}, and we could infer that similar results can be obtained by changing the death rate of CSC (d_1). Actually, the steady state was achieved under a balance between CSCs self-renewal and death. Indeed, variations of the other parameters, such as ω_{CSC} and ω_{PC}, did not result in persistent expansions of the tumor (though reaching another steady state of final volume quickly, data not shown). These results imply that the CSCs population plays a vital role in tumor progression, and more precisely, the CSCs division patterns decide the fate of the whole tumor, i.e., expansion, shrinking or maintenance. While the capacity for symmetric stem-cell self-renewal may confer enhanced regenerative capacity in normal tissues, it may also increase the risk of cancer (Morrison and Kimble, 2006). Moreover, our simulation results also indicate that genes that induce symmetric cell divisions could probably be oncogenes, which is in line with experimental observations (Lee et al., 2006; Regala et al., 2005a, 2005b). Note that in each case, the simulated percentage of CSCs (i.e., CSCs/total cell ratio) is also comparable to the ratio in literature, for example, in the steady state condition shown in Fig. 5A, the CSCs% = CSCs/(CSCs+PCs+TCs) $\approx 1/(1+33.2+66.4) \approx 1\%$.

4.2. CSC niche size determines the final tumor volume

In this section, we consider the effect of the CSCs niches on tumor growth. As discussed above, most of the CSCs divide symmetrically at the early stage of tumor, when most of the niches

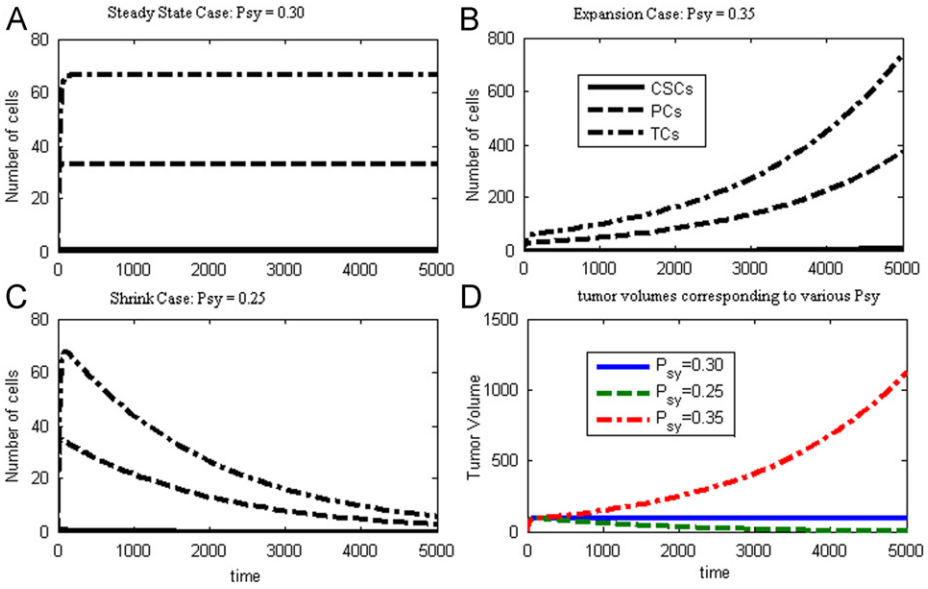

Fig. 5. The effect of the symmetric division probability (P_{sy}) on the tumor growth: (A) at an intermediate value, the tumor reaches its steady state with constant numbers of CSCs, PCs and TCs; (B) output from a higher value of P_{sy}, showing an expansion of the three populations over time; (C) output from a lower value of P_{sy}, showing a decrease of the three populations over time after a transient expansion at the early stage. In (D), green dashed, blue solid and red dash-dotted lines represent the tumor volumes over time in the case of $P_{sy}=0.25$, $P_{sy}=0.3$ and $P_{sy}=0.35$, respectively. (For interpretation of the references to color in this figure legend, the reader is referred to the web version of this article.)

are free. As the expansion of CSCs population, the probability of symmetric division will decrease. This assumption is derived from the investigation of embryonic development. For example, both neural and epidermal cells change from primarily symmetric divisions that expand stem-cell pools during early embryonic development to primarily asymmetric divisions that expand differentiated cells in the mid and late gestation (Morrison and Kimble, 2006). Therefore, the relationship between the CSCs number and P_{sy} can be described by a sigmoid curve as shown in Fig. 2. To study the effect of the niche size on the tumor growth, we varied the value for N_{niche}. For a certain value of N_{niche}, a steady state of tumor volume will probably be obtained after a dynamic selection of P_{sy}. Our simulation results are shown in Fig. 6, from which we can see that the tumor reached its steady state after a certain time in all three individual simulations. Moreover, our simulation results show that the final volume of tumor is correlated to the number of niches, that is, a larger number of niches would result in a tumor with larger volume. A more interesting thing is that the growth rate of the tumor at the early stage is larger if there is less niches. Thus, for a larger number of niches, the tumor grows at a slower rate, while the final tumor volume is larger. This implies that these tumors may be more dangerous even if they are difficult to be detected at the early stage.

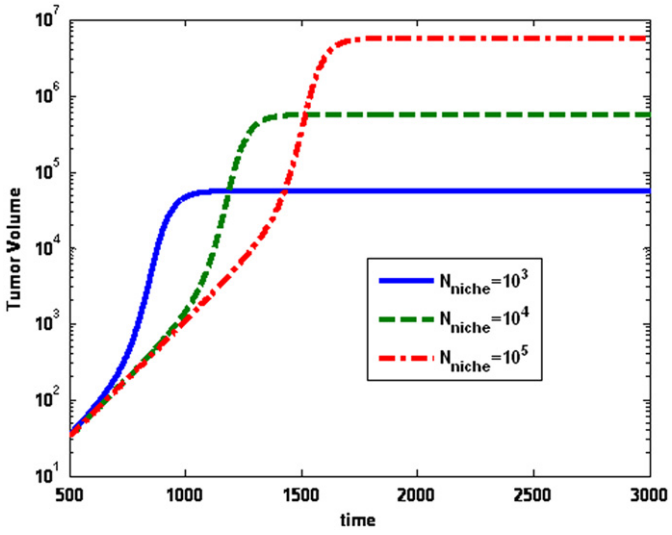

Fig. 6. The effect of niche size on the tumor growth. As the size of the niche increases, the tumor reaches its steady state more slowly, but resulting in a larger final volume.

4.3. CSC niches play an important role in cancer recurrence

Here, we simulated the tumor response to different theoretical treatments. First, we considered the situation that the niche was not included and the tumor would reach its steady stage in the absence of treatments. Therefore, we used the same parameters shown in Table 1 with the probability of symmetric division $P_{sy}=0.3$. Conventional methods of treatment, e.g., chemotherapy and radiotherapy, are usually aiming at tumor regression, which is thought to kill PCs and TCs, while sparing CSCs and resulting in recurrences of tumor. To model conventional therapies, we decreased the number of PCs and TCs by 90% after reaching the steady state (here, $t=200$). For the therapies targeting the CSCs, we set N_{CSC} to 10% of the value before the treatment. The simulation results in Fig. 7A show that various therapies resulted in distinct tumor growth. While a transient decrease was observed in the case of conventional therapy, the tumor would again expand to the original volume; however, for treatment targeting CSCs, the tumor would shrink to a smaller volume and never grows back to the volume before treatment, which implies the efficiency of treatment.

We next considered the situation that included the niche. The parameters used were the same as the previous case. The theoretical effects of treatments were also the same as the previous simulation: for conventional therapies, 90% of PCs and TCs would be killed; for the new treatment that targets CSCs, 90% of CSCs would be killed. The simulation results are shown in Fig. 7B, from

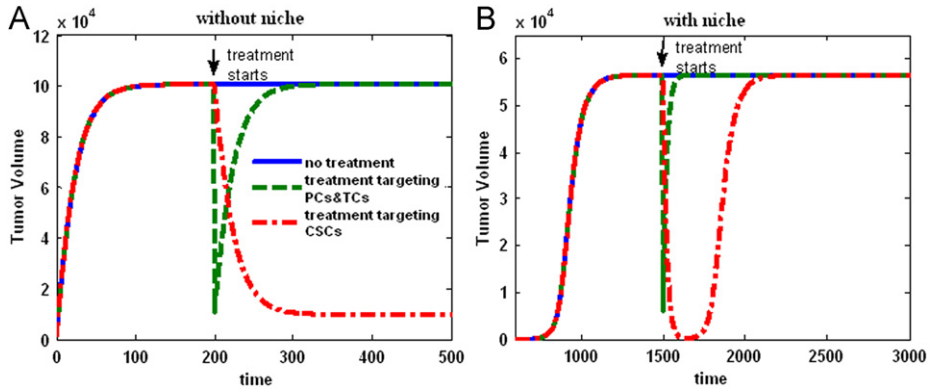

Fig. 7. Simulations of tumor response to treatments without (A) and with niche (B). In both cases, the solid blue lines represent the control condition where no treatment is imposed; the dashed green lines results from treatment targeting PCs and TCs; the dash-dotted red lines describe the changes of the tumor volume for a treatment targeting CSCs. Specially in (A), while conventional therapies result in a transient shrinking and then a recurrence of the tumor, the treatment targeting CSCs successfully diminish the tumor volume; in (B) the conventional therapies again result in a transient shrinking and then a faster recurrence of tumor; the treatment targeting CSCs diminishes the tumor to a smaller volume, but a slower recurrence of tumor is also observed. (For interpretation of the references to color in this figure legend, the reader is referred to the web version of this article.)

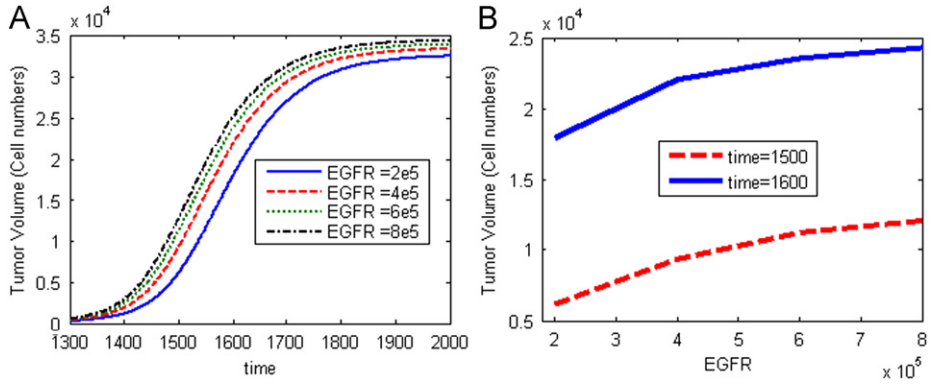

Fig. 8. Simulated tumor growth with various total number of EGFR per cell. (A) compares the cell population growth. (B) shows the relationships between total EFGR numbers and tumor growth data (points taken from (A) at time=1500 and time=1600).

which we can see that the conventional treatments resulted in a transient shrinking and a subsequent recurrence quickly. For the treatments targeting CSCs, although the tumor was reduced to a small volume after treatment, the tumor recurrence to the original volume was also observed, albeit much slower than the case with conventional treatment. These findings imply the underlying effect of niche on the maintenance of the CSCs population and on the recurrence of breast cancer. The number of CSCs would increase again, if the niches have not been destroyed or the CSCs were not eliminated completely. This result again suggests the niches as a potential and more important target for the novel therapies to cure cancers.

4.4. The effect of EGFR on tumor dynamics

As described previously, the total number of EGFR per cell varies in a large range due to different cell lines. In addition, EGFR expression is much higher in CSCs than it is in other tumor cells (Magnifico et al., 2009). To understand the relationship between the total number of EGFR and the tumor growth, we simulated the tumor volumes over time by changing the parameter value for the total number of EGFR found in PCs and TCs from 200,000 to 800,000, while the total EGFR in CSCs was assume to be 800,000. The simulation results are shown in Fig. 8, which shows a positive correlation between tumor growth and EGFR concentration, i.e., the tumor grows faster and the final volume of the tumor is also larger as the total number of EGFR increases (Fig. 8A). In addition, we also note that our model predicts that the dose-response of tumor to total EGFR approaches a saturation function as the total EGFR number increases. As a result, increasing the level of total EGFR beyond a maximum number (i.e., a threshold) will not significantly alter the tumor growth rates and final volumes. As shown in Fig. 8B, the dose-response dependence of cell proliferation rates on the total EGFR number becomes weaker (a smaller slope).

4.5. Tumor response to various treatments with both niche and signaling pathway

As described in Fig. 3, we will consider the tumor response to different treatments in this section. Similarly to the simulation in Section 4.3, we used the parameters in Table 1 as the case of control without treatment. The tumor again reached its steady stage after a certain time, with a constant volume and CSC percentage. Then, conventional treatments (e.g., doxorubicin) was imposed and, for simplicity, we assumed that only the death rates of PC and TC cells was increased by an additional 50% in the case of standard dose. Our simulation results in Fig. 9 show that conventional treatments result in a decrease of tumor volume, and an increased CSC percentage, which is in agreement with the findings of Li et al. (2008) as shown in Fig. 9C and D. While PCs and TCs that comprise the bulk of tumor were killed, the CSCs were left, which accounts for the tumor relapsed as soon as the treatments stopped.

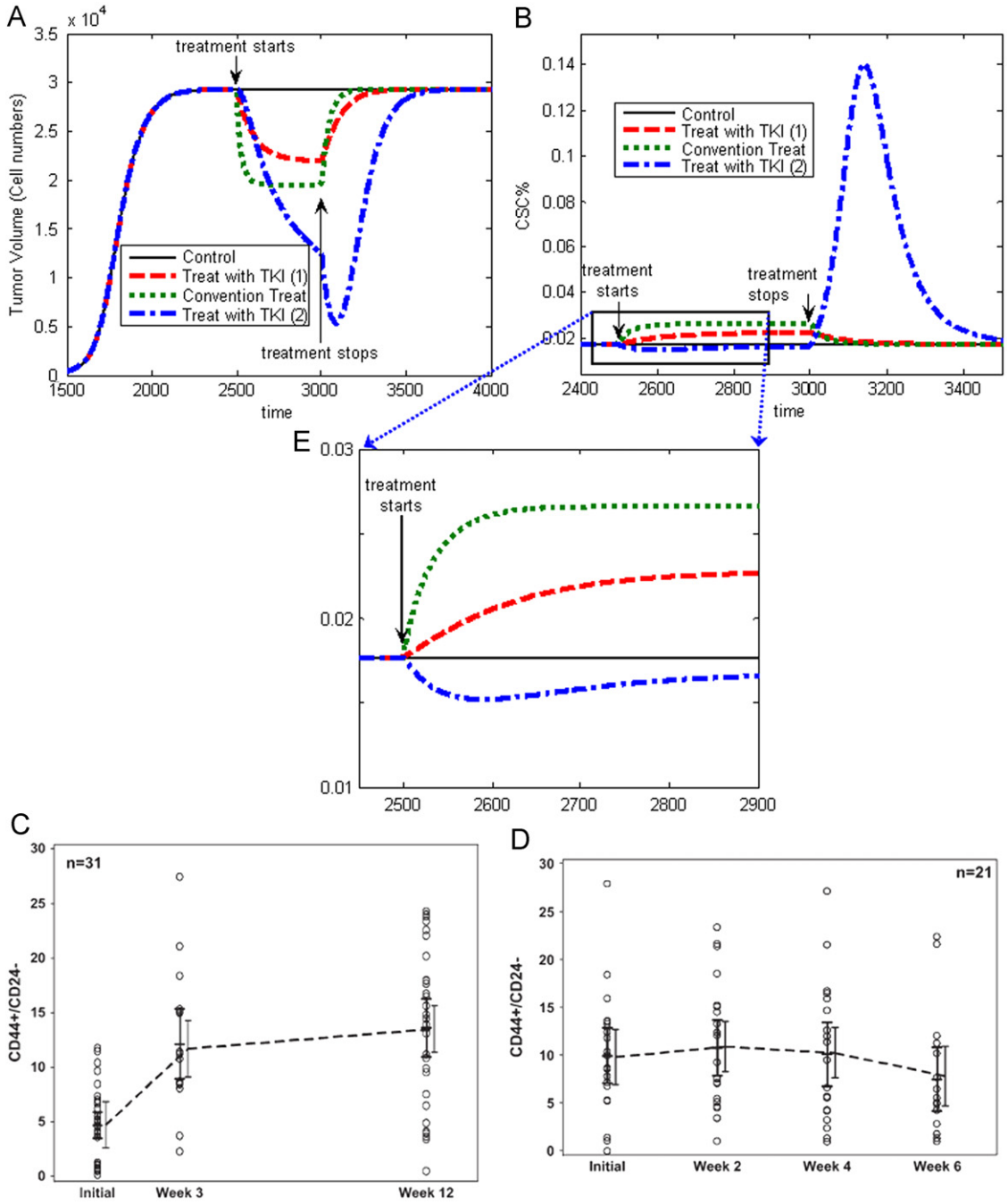

Fig. 9. Simulated response of tumor to different treatments. (A) Shows the tumor volumes over time and (B) shows the CSC percentage over time without treatment (black solid line), with conventional treatment (green dotted line) and with the treatment of TKIs. Note, while the red dashed lines represent TKIs treatments that inhibit proliferation and induce apoptosis, the blue dash-dotted lines shows TKIs treatments including the change of self-renew patterns as well. (C) and (D) show the percentages of $CD44^+/CD24^-$ cells, which are thought to be CSCs, under treatments of chemotherapy and lapatinib, respectively, figures are derived from Li et al. (2008). (E) zoomed in on the treatment part of (B). Comparison of (C), (D) and (E) shows a consistency between experimental data and simulation results. (For interpretation of the references to color in this figure legend, the reader is referred to the web version of this article.)

For the treatments with lapatinib on patients with HER2-positive tumors, the initial concentration of TKIs was 1.0×10^{-9} M. The effective EGF–EGFR complex is decreased due to the binding of TKIs to the intracellular domain of EGFR. Since we assumed that the amount of effective EFG-EGFR is related to the rates of proliferation and apoptosis, the presence of TKIs simultaneously represses the proliferation and induces the death of CSC, PC and TC cells (Fig. 3). The simulation results are shown in Fig. 9 with dashed lines. While the repression of tumor volume is obvious, the increased CSC percentage is not so significant (Fig. 9B). Indeed, Li et al. (2008) found that, in addition to the repression of tumor volume, the treatment with lapatinib led to a non-statistically significant decrease in the percentage of $CD44^+/CD24^{-/low}$ cells that are thought to be cancer stem cells. This implied the hypothesis that TKIs also have an effect changing the self-renewal patterns by shifting symmetric division to asymmetric division.

To test this hypothesis, in our mathematical model, in addition to calculating the parameter values for proliferation rates and death rates with Eqs. (9) and (10), respectively, we also changed the parameter that decides division pattern of CSC when the TKIs

treatment is imposed. As a first approximation, we simply multiplied the term $P_{sy}(N_{CSC})$ with a value of 0.25 to model the shift of CSC division from symmetric to asymmetric pattern. The simulation results are shown in Fig. 9 with dash-dotted lines. This time, not only decrease of tumor volume but also the slight decrease of CSC percentage is observed when the TKI treatment is imposed, which is consistent with the finding of Li et al. (2008). For the percentage of cancer stem cells (or tumor-initiating cells) before and during treatments, comparison between simulation and experimental data can be seen in Fig. 9C–E, where Fig. 9E zoomed in on the treatment part of Fig. 9B. From the figure we can see that while conventional treatment increased the CSC% by near 50% (from 1.8% to 2.7%), TKI treatment caused no significant change in CSC%, or even reduced the CSC% slightly.

Furthermore, it is worth noting that even after treatment stops, the tumor volume still decreases for a certain time, and a sharp increase of CSC percentage occurs after the treatment. These can be understood in this way: when the treatment stops, both the tumor volume and CSC numbers are small, therefore, most of CSC cells shift back to symmetric division in order to first increase the CSC population and then expand the tumor volume. Thus, despite an increase of the CSC population (a small fraction of total tumor volume), a decrease of PC and TC (a major component of total tumor volume) continues, resulting in a repression of the total volume of tumor, but an increase of the CSC percentage.

5. Discussion and conclusion

The field of cancer research is undergoing a transformation with the concept that the tumors are also initiated and driven by a small group of CSCs, which is also known as the cancer stem cell hypothesis. The presence of CSCs is firstly demonstrated for hematopoietic neoplasm (Wang and Dick, 2005), and there is currently increasing evidence that CSCs exist in solid tumors as well, including breast carcinoma (Dick, 2003), brain tumors (Singh et al., 2004) and colon carcinoma (O'Brien et al., 2007; Ricci-Vitiani et al., 2007). Moreover, the concept of the CSCs niche was proposed recently, and becomes an important topic in cancer research now.

In this paper we proposed an improved compartment model that describes the composition of breast cancer by using an ordinary differential equations system, providing insight into the cellular kinetic mechanisms that drive the tumor growth. Firstly, the proposed model addressed the effect of CSCs on the tumor progression: the maintenance of CSCs through the symmetric division is the driving force for the tumor growth, and the balance of the self-renewal and the loss of CSCs results in the steady state of a tumor. The loss of CSCs could be occurred via apoptosis, differentiation or cell death caused by therapies. If the self-renewal is faster than the loss, then CSCs population will expand, subsequently causing the expansion of tumor volume. In contrast, if the loss overcomes the self-renewal, then repression of the tumor will occur, which suggests the successful drug treatment should increase the loss or decrease the self-renewal of CSCs. The CSCs division patterns, however, cannot be constants in either in vitro or in vivo conditions; rather they are dependent on the surrounding environment that is changing all the time. Therefore, we also considered the role of cancer stem cell niche in our model. By describing the division patterns as functions of the niche size and CSCs number, we incorporated the niche into the ODE system and studied the role of the niche in driving the tumor progression. Our simulation results showed that a larger size of niche gives birth to a larger population of CSCs, and subsequently results in a larger tumor. Interestingly, however, a bigger niche leads to a slower rather than faster growth of the tumor. This may be caused by a larger probability of symmetric division of CSC at the early stage and a smaller growth of PCs and TCs that are responsible for the bulk of the tumor volume.

Similar work on the tumor population with respect to the division patterns has also been done by other groups (Boman et al., 2007; Dingli et al., 2007). Boman et al. investigated the cellular mechanisms and kinetics that occur in stem cell population during colorectal cancer development. They found that an increased symmetric stem cell division would result in exponential growth of all cellular populations in their model, which is consistent with our result. Dingli et al. (Boman et al., 2007; Dingli et al., 2007) developed a mathematical model to illustrate the impact of mutations that regulate the symmetric stem cell division on the development of tumors. While considering the symmetric and asymmetric division as well, their work focused on the mutation within the stem cells and the competition between stem cells and cancer stem cells. The incorporation of the EGFR signaling pathways in our model is an approximation, while a more detailed mathematical model was proposed in the work of Eladdadi and Isaacson (2008). Indeed, their work was also a simplification of effects of the whole signaling pathways on cellular properties. More recently, Agur et al. (2010) and Kirnasovsky et al. (2008) published two papers where symmetric and asymmetric divisions of stem cells were also considered. Both papers studied the stem cell development with a feedback from the environment, i.e., Quorum Sensing concept, however, while the first one focused on the intercellular communication by using a discrete cellular automata model (Agur et al., 2010), the other one mathematically analyzed the intracellular and micro-environmental protein interactions (Kirnasovsky et al., 2008). Their work is more specific while we are trying to incorporate them together though in a simplified way.

However, the limitations of our work are also obvious. For example, our simulation is largely based on theoretical assumption, due to the lack of experimental data. The cancer stem cell niche itself is a very new concept and just defined as a functional structure. It is currently difficult to measure the size of the niche, not to mention physically and physiologically controlling the niche. The relationship between the symmetric division probability, niche size and CSCs also needs further improvement, while we used a general sigmoid curve to describe it in our work. In addition, the molecules in the niche are important for maintaining the signaling pathways that account for the balance between self-renewal and differentiation of CSCs (Li and Neaves, 2006). Together with the subcellular signaling pathway information, e.g., Wnt (Alonso and Fuchs, 2003; Pinto and Clevers, 2005; Reya and Clevers, 2005), Notch (Brennan and Brown, 2003) and Hedgehog (Liu et al., 2006), understanding quantitatively how these molecules and nutrients distribute, diffuse and are utilized in the niche will provide insight into a more detailed mechanism for the CSCs fate. We are now building a mathematical model that describes the crosstalk between Notch, which is involved in the regulation of cellular properties of stem cells, and HER2 signaling pathways, with a focus on the interactions between molecular dynamics at the protein level. It will be incorporated into this proposed model as a more precise link between signaling pathways and cellular properties.

Furthermore, for application to development of breast cancer in this work, the compartment model per se has some limitations. As described above, the goal of our work is to incorporate the most important concepts while keeping the model as simple as possible. We therefore classify all breast cancer cells into three groups, i.e., CSC, PCs and TCs, which is certainly an approximation of the system. While each compartment is assumed to be a homogenous entity, the cells in each single compartment are heterogeneous in biological function. Therefore, the compartment model can only serve as a tool for studying macroscopic phenomena so that we cannot look into the behavior of each single cell. Extensions of this

model, for example, a more mechanistic-based method of modeling the function of signaling pathways, are obviously needed. More detailed modeling of the effect of niche should also be necessary in the future, especially the interaction among CSC/PC/TC cells and stromal cells, as well as the secreted factors from different cells. These dynamics may include both positive and negative feedback mechanisms, interplay between environmental factors and genetic functions.

In summary, our mathematical model studied the impact of CSCs division pattern on the tumor expansion, incorporated the effect of CSCs niche, and integrated a simplified effect of EGFR signaling pathway as well. Our model is one of rare work with attempt to integrate the cancer stem cell niche to a mathematical model and provides a primary simulation results on the effect of a niche on tumor growth, and the validation of the proposed model is done by comparing simulation results with clinical studies. Simulations with our model suggest the important roles of the symmetric division of CSCs, niche size and over-expression of EGFR in tumor progression. The simulated responses of tumor to drug treatments suggest that future therapies should be either designed to effectively reduce or destroy the CSC niche, or block signaling pathways by tyrosine kinase inhibitors.

Acknowledgments

This work is partially funded by U54CA149196, and the authors would like to acknowledge the valuable discussions from Drs. Hong Zhao, Xiaofeng Xia, and Kemi Cui at the Center for Bioengineering and Informatics of the Methodist Hospital Research Institute.

References

Adams, G.B., Scadden, D.T., 2006. The hematopoietic stem cell in its place. Nat. Immunol. 7, 333–337.
Adams, G.B., Martin, R.P., Alley, I.R., Chabner, K.T., Cohen, K.S., Calvi, L.M., Kronenberg, H.M., Scadden, D.T., 2007. Therapeutic targeting of a stem cell niche. Nat. Biotechnol. 25, 238–243.
Agur, Z., Kogan, Y., Levi, L., Harrison, H., Lamb, R., Kirnasovsky, O.U., Clarke, R.B., 2010. Disruption of a Quorum Sensing mechanism triggers tumorigenesis: a simple discrete model corroborated by experiments in mammary cancer stem cells. Biol. Direct 5, 20.
Alonso, L., Fuchs, E., 2003. Stem cells in the skin: waste not, Wnt not. Genes Dev. 17, 1189–1200.
Al-Hajj, M., Clarke, M.F., 2004. Self-renewal and solid tumor stem cells. Oncogene 23, 7274–7282.
Anderson, A.R., Chaplain, M.A., 1998. Continuous and discrete mathematical models of tumor-induced angiogenesis. Bull. Math. Biol. 60, 857–899.
Anderson, K.C., 2007. Targeted therapy of multiple myeloma based upon tumor-microenvironmental interactions. Exp. Hematol. 35, 155–162.
Araujo, R.P., McElwain, D.L., 2004. A history of the study of solid tumour growth: the contribution of mathematical modelling. Bull. Math. Biol. 66, 1039–1091.
Athale, C.A., Deisboeck, T.S., 2006. The effects of EGF-receptor density on multiscale tumor growth patterns. J. Theor. Biol. 238, 771–779.
Baumann, M., Krause, M., Hill, R., 2008. Exploring the role of cancer stem cells in radioresistance. Nat. Rev. Cancer 8, 545–554.
Birtwistle, M.R., Hatakeyama, M., Yumoto, N., Ogunnaike, B.A., Hoek, J.B., Kholodenko, B.N., 2007. Ligand-dependent responses of the ErbB signaling network: experimental and modeling analyses. Mol. Syst. Biol. 3, 144.
Bjerknes, M., Cheng, H., 1999. Clonal analysis of mouse intestinal epithelial progenitors. Gastroenterology 116, 7–14.
Boman, B.M., Wicha, M.S., Fields, J.Z., Runquist, O.A., 2007. Symmetric division of cancer stem cells—a key mechanism in tumor growth that should be targeted in future therapeutic approaches. Clin. Pharmacol. Ther. 81, 893–898.
Brennan, K., Brown, A.M., 2003. Is there a role for Notch signalling in human breast cancer? Breast Cancer Res. 5 69–75.
Byrne, H.M., Chaplain, M.A., 1995. Growth of nonnecrotic tumors in the presence and absence of inhibitors. Math. Biosci. 130, 151–181.
Calabrese, C., Poppleton, H., Kocak, M., Hogg, T.L., Fuller, C., Hamner, B., Oh, E.Y., Gaber, M.W., Finklestein, D., Allen, M., Frank, A., Bayazitov, I.T., Zakharenko, S.S., Gajjar, A., Davidoff, A., Gilbertson, R.J., 2007. A perivascular niche for brain tumor stem cells. Cancer Cell 11, 69–82.
Chaplain, M.A., McDougall, S.R., Anderson, A.R., 2006. Mathematical modeling of tumor-induced angiogenesis. Annu. Rev. Biomed. Eng. 8, 233–257.
Clarke, M.F., Dick, J.E., Dirks, P.B., Eaves, C.J., Jamieson, C.H., Jones, D.L., Visvader, J., Weissman, I.L., Wahl, G.M., 2006. Cancer stem cells–perspectives on current status and future directions: AACR Workshop on cancer stem cells. Cancer Res. 66, 9339–9344.
Costa, D.B., Halmos, B., Kumar, A., Schumer, S.T., Huberman, M.S., Boggon, T.J., Tenen, D.G., Kobayashi, S., 2007. BIM mediates EGFR tyrosine kinase inhibitor-induced apoptosis in lung cancers with oncogenic EGFR mutations. PLoS Med. 4, 1669–1679 discussion 1680.
Cristini, V., Lowengrub, J., Nie, Q., 2003. Nonlinear simulation of tumor growth. J. Math. Biol. 46, 191–224.
Cristini, V., Frieboes, H.B., Gatenby, R., Caserta, S., Ferrari, M., Sinek, J., 2005. Morphologic instability and cancer invasion. Clin. Cancer Res. 11, 6772–6779.
d'Onofrio, A., Tomlinson, I.P., 2007. A nonlinear mathematical model of cell turnover, differentiation and tumorigenesis in the intestinal crypt. J. Theor. Biol. 244, 367–374.
Dick, J.E., 2003. Breast cancer stem cells revealed. Proc. Natl. Acad. Sci. USA 100, 3547–3549.
Dingli, D., Traulsen, A., Michor, F., 2007. (A)symmetric stem cell replication and cancer. PloS Comput. Biol. 3, e53.
El-Kareh, A.W., Secomb, T.W., 2003. A mathematical model for cisplatin cellular pharmacodynamics. Neoplasia 5, 161–169.
Eladdadi, A., Isaacson, D., 2008. A mathematical model for the effects of HER2 overexpression on cell proliferation in breast cancer. Bull. Math. Biol. 70, 1707–1729.
Frieboes, H.B., Edgerton, M.E., Fruehauf, J.P., Rose, F.R., Worrall, L.K., Gatenby, R.A., Ferrari, M., Cristini, V., 2009. Prediction of drug response in breast cancer using integrative experimental/computational modeling. Cancer Res. 69, 4484–4492.
Gan, H.K., Walker, F., Burgess, A.W., Rigopoulos, A., Scott, A.M., Johns, T.G., 2007. The epidermal growth factor receptor (EGFR) tyrosine kinase inhibitor AG1478 increases the formation of inactive untethered EGFR dimers. Implications for combination therapy with monoclonal antibody 806. J. Biol. Chem. 282, 2840–2850.
Ganguly, R., Puri, I.K., 2006. Mathematical model for the cancer stem cell hypothesis. Cell Prolif. 39, 3–14.
Gordan, J.D., Bertout, J.A., Hu, C.J., Diehl, J.A., Simon, M.C., 2007. HIF-2alpha promotes hypoxic cell proliferation by enhancing c-myc transcriptional activity. Cancer Cell 11, 335–347.
Gustafsson, M.V., Zheng, X., Pereira, T., Gradin, K., Jin, S., Lundkvist, J., Ruas, J.L., Poellinger, L., Lendahl, U., Bondesson, M., 2005. Hypoxia requires notch signaling to maintain the undifferentiated cell state. Dev. Cell 9, 617–628.
Hendriks, B.S., Opresko, L.K., Wiley, H.S., Lauffenburger, D., 2003. Quantitative analysis of HER2-mediated effects on HER2 and epidermal growth factor receptor endocytosis: distribution of homo- and heterodimers depends on relative HER2 levels. J. Biol. Chem. 278, 23343–23351.
Ho, A.D., 2005. Kinetics and symmetry of divisions of hematopoietic stem cells. Exp. Hematol. 33, 1–8.
Holz, M., Fahr, A., 2001. Compartment modeling. Adv. Drug Deliv. Rev. 48, 249–264.
Hu, C.J., Wang, L.Y., Chodosh, L.A., Keith, B., Simon, M.C., 2003. Differential roles of hypoxia-inducible factor 1alpha (HIF-1alpha) and HIF-2alpha in hypoxic gene regulation. Mol. Cell Biol. 23, 9361–9374.
Johnston, M.D., Edwards, C.M., Bodmer, W.F., Maini, P.K., Chapman, S.J., 2007. Mathematical modeling of cell population dynamics in the colonic crypt and in colorectal cancer. Proc. Natl. Acad. Sci. USA 104, 4008–4013.
Joyce, J.A., 2005. Therapeutic targeting of the tumor microenvironment. Cancer Cell 7, 513–520.
Kirnasovsky, O., U., Kogan, Y., Agur, Z., 2008. Analysis of a mathematical model for the molecular mechanism of fate decision in mammary stem cells. Math. Model. Nat. Phenom. 3, 78–89.
Kong, A., Calleja, V., Leboucher, P., Harris, A., Parker, P.J., Larijani, B., 2008. HER2 oncogenic function escapes EGFR tyrosine kinase inhibitors via activation of alternative HER receptors in breast cancer cells. PLoS ONE 3, e2881.
Kopper, L., Hajdu, M., 2004. Tumor stem cells. Pathol. Oncol. Res. 10, 69–73.
Korkaya, H., Paulson, A., Iovino, F., Wicha, M.S., 2008. HER2 regulates the mammary stem/progenitor cell population driving tumorigenesis and invasion. Oncogene 27, 6120–6130.
Lechler, T., Fuchs, E., 2005. Asymmetric cell divisions promote stratification and differentiation of mammalian skin. Nature 437, 275–280.
Lee, C.Y., Robinson, K.J., Doe, C.Q., 2006. Lgl, Pins and aPKC regulate neuroblast self-renewal versus differentiation. Nature 439, 594–598.
Li, L., Neaves, W.B., 2006. Normal stem cells and cancer stem cells: the niche matters. Cancer Res. 66, 4553–4557.
Li, X., Lewis, M.T., Huang, J., Gutierrez, C., Osborne, C.K., Wu, M.F., Hilsenbeck, S.G., Pavlick, A., Zhang, X., Chamness, G.C., Wong, H., Rosen, J., Chang, J.C., 2008. Intrinsic resistance of tumorigenic breast cancer cells to chemotherapy. J. Natl. Cancer Inst. 100, 672–679.
Liu, S., Dontu, G., Mantle, I.D., Patel, S., Ahn, N.S., Jackson, K.W., Suri, P., Wicha, M.S., 2006. Hedgehog signaling and Bmi-1 regulate self-renewal of normal and malignant human mammary stem cells. Cancer Res. 66, 6063–6071.
Magnifico, A., Albano, L., Campaner, S., Delia, D., Castiglioni, F., Gasparini, P., Sozzi, G., Fontanella, E., Menard, S., Tagliabue, E., 2009. Tumor-initiating cells of HER2-positive carcinoma cell lines express the highest oncoprotein levels and are sensitive to trastuzumab. Clin. Cancer Res. 15, 2010–2021.
Michor, F., Hughes, T.P., Iwasa, Y., Branford, S., Shah, N.P., Sawyers, C.L., Nowak, M.A., 2005. Dynamics of chronic myeloid leukaemia. Nature 435, 1267–1270.
Monod, J., 1949. The Growth of Bacterial Cultures. Annu. Rev. Microbiol. 3, 371–394.
Morrison, S.J., Kimble, J., 2006. Asymmetric and symmetric stem-cell divisions in development and cancer. Nature 441, 1068–1074.

Narbonne, P., Roy, R., 2006. Regulation of germline stem cell proliferation downstream of nutrient sensing. Cell Div. 1, 29.
O'Brien, C.A., Pollett, A., Gallinger, S., Dick, J.E., 2007. A human colon cancer cell capable of initiating tumour growth in immunodeficient mice. Nature 445, 106–110.
Paguirigan, A., Beebe, D.J., Alexander, C.M., 2007. Simulating mouse mammary gland development: cell ageing and its relation to stem and progenitor activity. Cell Prolif. 40, 106–124.
Paulus, U., Potten, C.S., Loeffler, M., 1992. A model of the control of cellular regeneration in the intestinal crypt after perturbation based solely on local stem cell regulation. Cell Prolif. 25, 559–578.
Pinto, D., Clevers, H., 2005. Wnt control of stem cells and differentiation in the intestinal epithelium. Exp. Cell Res. 306, 357–363.
Potten, C.S., Booth, C., Pritchard, D.M., 1997. The intestinal epithelial stem cell: the mucosal governor. Int. J. Exp. Pathol. 78, 219–243.
Regala, R.P., Weems, C., Jamieson, L., Copland, J.A., Thompson, E.A., Fields, A.P., 2005a. Atypical protein kinase Ciota plays a critical role in human lung cancer cell growth and tumorigenicity. J. Biol. Chem. 280, 31109–31115.
Regala, R.P., Weems, C., Jamieson, L., Khoor, A., Edell, E.S., Lohse, C.M., Fields, A.P., 2005b. Atypical protein kinase C iota is an oncogene in human non-small cell lung cancer. Cancer Res. 65, 8905–8911.
Reya, T., Clevers, H., 2005. Wnt signalling in stem cells and cancer. Nature 434, 843–850.
Reya, T., Morrison, S.J., Clarke, M.F., Weissman, I.L., 2001. Stem cells, cancer, and cancer stem cells. Nature 414, 105–111.
Ribba, B., Colin, T., Schnell, S., 2006. A multiscale mathematical model of cancer, and its use in analyzing irradiation therapies. Theor. Biol. Med. Model. 3, 7.
Ricci-Vitiani, L., Lombardi, D.G., Pilozzi, E., Biffoni, M., Todaro, M., Peschle, C., De Maria, R., 2007. Identification and expansion of human colon-cancer-initiating cells. Nature 445, 111–115.
Scadden, D.T., 2006. The stem-cell niche as an entity of action. Nature 441, 1075–1079.
Shipitsin, M., Campbell, L.L., Argani, P., Weremowicz, S., Bloushtain-Qimron, N., Yao, J., Nikolskaya, T., Serebryiskaya, T., Beroukhim, R., Hu, M., Halushka, M.K., Sukumar, S., Parker, L.M., Anderson, K.S., Harris, L.N., Garber, J.E., Richardson, A.L., Schnitt, S.J., Nikolsky, Y., Gelman, R.S., Polyak, K., 2007. Molecular definition of breast tumor heterogeneity. Cancer Cell 11, 259–273.
Sinek, J.P., Sanga, S., Zheng, X., Frieboes, H.B., Ferrari, M., Cristini, V., 2009. Predicting drug pharmacokinetics and effect in vascularized tumors using computer simulation. J. Math. Biol. 58, 485–510.
Singh, S.K., Hawkins, C., Clarke, I.D., Squire, J.A., Bayani, J., Hide, T., Henkelman, R.M., Cusimano, M.D., Dirks, P.B., 2004. Identification of human brain tumour initiating cells. Nature 432, 396–401.
Timms, J.F., White, S.L., O'Hare, M.J., Waterfield, M.D., 2002. Effects of ErbB-2 overexpression on mitogenic signalling and cell cycle progression in human breast luminal epithelial cells. Oncogene 21, 6573–6586.
Tomlinson, I.P., Bodmer, W.F., 1995. Failure of programmed cell death and differentiation as causes of tumors: some simple mathematical models. Proc. Natl. Acad. Sci. USA 92, 11130–11134.
Visnjic, D., Kalajzic, Z., Rowe, D.W., Katavic, V., Lorenzo, J., Aguila, H.L., 2004. Hematopoiesis is severely altered in mice with an induced osteoblast deficiency. Blood 103, 3258–3264.
Visvader, J.E., Lindeman, G.J., 2008. Cancer stem cells in solid tumours: accumulating evidence and unresolved questions. Nat. Rev. Cancer 8, 755–768.
Vogel, C.L., Cobleigh, M.A., Tripathy, D., Gutheil, J.C., Harris, L.N., Fehrenbacher, L., Slamon, D.J., Murphy, M., Novotny, W.F., Burchmore, M., Shak, S., Stewart, S.J., Press, M., 2002. Efficacy and safety of trastuzumab as a single agent in first-line treatment of HER2-overexpressing metastatic breast cancer. J. Clin. Oncol. 20, 719–726.
Walker, M.R., Patel, K.K., Stappenbeck, T.S., 2009. The stem cell niche. J. Pathol. 217, 169–180.
Wang, J.C., Dick, J.E., 2005. Cancer stem cells: lessons from leukemia. Trends Cell Biol. 15, 494–501.
Woodward, W.A., Chen, M.S., Behbod, F., Alfaro, M.P., Buchholz, T.A., Rosen, J.M., 2007. WNT/beta-catenin mediates radiation resistance of mouse mammary progenitor cells. Proc. Natl. Acad. Sci. USA 104, 618–623.
Xie, T., Spradling, A.C., 2000. A niche maintaining germ line stem cells in the Drosophila ovary. Science 290, 328–330.
Zhang, J., Niu, C., Ye, L., Huang, H., He, X., Tong, W.G., Ross, J., Haug, J., Johnson, T., Feng, J.Q., Harris, S., Wiedemann, L.M., Mishina, Y., Li, L., 2003. Identification of the haematopoietic stem cell niche and control of the niche size. Nature 425, 836–841.
Zheng, X., Wise, S.M., Cristini, V., 2005. Nonlinear simulation of tumor necrosis, neo-vascularization and tissue invasion via an adaptive finite-element/level-set method. Bull. Math. Biol. 67, 211–259.